

Dark matter flow dataset Part I: Halo-based statistics from cosmological N-body simulation

Zhijie (Jay) Xu,¹★

¹Physical and Computational Sciences Directorate, Pacific Northwest National Laboratory; Richland, WA 99352, USA

Accepted XXX. Received YYY; in original form ZZZ

ABSTRACT

Dark matter (DM), if exists, is believed to be cold, collisionless, dissipationless, non-baryonic, barely interacting with baryonic matter except through gravity, and sufficiently smooth on large scales with a fluid-like behavior. The flow of dark matter can be best described by a self-gravitating collisionless fluid dynamics (SG-CFD). The statistics of dark matter density, velocity, acceleration, energy, momentum, and their redshift evolution play essential roles for structure formation and evolution. These information can be systematically extracted from cosmological N-body simulations by either i) a structural (halo-based) or ii) a statistical (correlation-based) approach. In this halo-based statistical dataset, i) all halos in N-body system are identified with all particles divided into halo and out-of-halo particles; ii) halos are grouped into halo groups including all halos of the same mass (m_h); iii) the redshift (z) and mass scale (m_h) dependence of all halo properties (momentum, energy, size, shape, velocity, acceleration, etc.) are presented.

Key words: Cosmology; Dark matter; N-body simulations; Halo-based statistics;

1 INTRODUCTION

The spatial distribution of dark matter at statistically steady state consists of distinct halos of different size. Statistical description of the entire system requires full knowledge of the distribution of halo mass, the distribution of particles within individual halos, and the spatial clustering of halos. The halo description of the statistically steady state for self-gravitating collisionless dark matter flow can be a direct result of long-range interaction to maximize system entropy (Xu 2021c). This dataset presents the halo-based statistics for dark matter flow that was used to develop the theory including

- (i) Inverse mass cascade of dark matter flow, random walk in mass space, and halo mass functions (Xu 2021a,e)
- (ii) Halo deformation, halo concentration, energy, surface tension, size, density profiles, and equation of state (Xu 2021b)
- (iii) Inverse cascade of kinetic energy, direct cascade of potential energy, and effects of halo shape on energy cascade (Xu 2021f)
- (iv) Halo energy, radial and angular momentum, spin parameter, and integral constants of motion (Xu 2022d)
- (v) Halo mean flow, velocity dispersion and energy transfer between mean flow and dispersion (random motion) (Xu 2022c)
- (vi) Halo-based non-projection approach for density and velocity distributions in dark matter flow (Xu 2022e)

along with three applications of dark matter flow

- (i) Predicting Dark matter particle mass and properties from energy cascade in dark matter flow (Xu 2022f)

- (ii) Origin of MOND acceleration and deep-MOND from acceleration fluctuation and energy cascade in dark matter flow (Xu 2022g)
- (iii) Baryonic-to-halo mass relation from mass and energy cascade in dark matter flow (Xu 2022h)

Presentation slides accompanying this dataset, "A comparative study of dark matter flow & hydrodynamic turbulence and its applications", can be found at (Xu 2022a). A relevant dataset for correlation-based statistics of dark matter flow can be found at (Xu 2022b).

2 N-BODY SIMULATIONS AND NUMERICAL DATA

The simulation data used to generate this dataset is public available from large-scale N-body simulations carried out by the Virgo consortium. A comprehensive description of the data can be found in (Frenk et al. 2000). Current study is carried out using simulations with $\Omega_0 = 1$ and the standard CDM power spectrum (SCDM) to focus on the matter-dominant (Einstein–de Sitter) gravitational collapse. The same set of data has been widely used in a number of studies from clustering statistics to the formation of cluster halos in large scale environments, and halo abundances and mass functions. Key simulation parameters are provided in Table 1.

The friends-of-friends algorithm (FOF) was used to identify all halos from the simulation data that depends only on a dimensionless parameter b , which defines the linking length $b(N/V)^{-1/3}$, where N is the total number of particles and V is the volume of simulation box. Halos were identified with a linking length parameter of $b = 0.2$ in this work. All halos identified from simulation data were grouped into halo groups of different size according to halo mass m_h (or in terms of n_p , the number of particles in halo), where $m_h = n_p m_p$. The total mass for a halo group of mass m_h is $m_g = m_h n_h$, where n_h is the number of halos in each group. Figure 1 is a schematic plot

★ E-mail: zhijie.xu@pnnl.gov; zhijiexu@hotmail.com

Table 1. Numerical parameters of N-body simulation

Run	Ω_0	Λ	h	Γ	σ_8	L (Mpc/h)	N_P	m_P M_\odot/h	l_{soft} (Kpc/h)
SCDM1	1.0	0.0	0.5	0.5	0.51	239.5	256^3	2.27×10^{11}	36

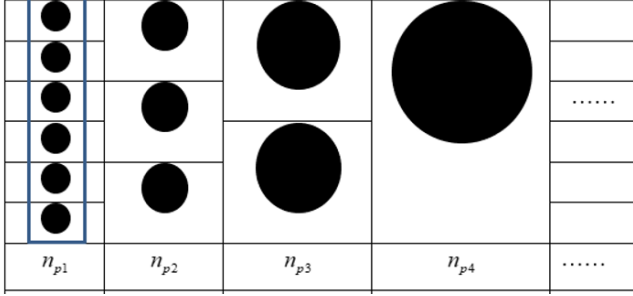


Figure 1. A schematic plot of group of halos of different size. Halos are grouped and sorted according to the number of particles $n_P = m_h/m_P$ in halo, where m_P is particle mass or mass resolution of N-body simulation. Every halo group includes all halos of the same mass m_h . Halo-based statistics in this dataset is presented as the average or standard deviation for all halos in the same group. Therefore, various halo properties are presented as functions of halo mass m_h and redshift z .

of the halo picture by sorting all halos according to their sizes from the smallest to largest. Each column in Fig. 1 is a group of halos of the same size.

3 OVERVIEW

Halo-based statistical data in this package was generated from large scale N-body simulations and saved in a format of CSV file.

3.1 Data Availability

The data underlying this article are available in Zenodo at [Dark matter flow dataset Part I: Halo-based statistics from cosmological N-body simulation](#).

- ☑ All data **are** publicly available.
- Some data **cannot be made** publicly available.
- No data **can be made** publicly available.

3.2 Dataset list

Table 2 lists all data files included in this dataset. Every data file presents the mass and redshift dependence of one halo variable with symbols also listed in the same table. The physical meaning of that variable can be found from the name of file. More details (definition, units, relevant publications, equations, and figures) can be found in the header of each data file.

REFERENCES

- Frenk C. S., et al., 2000, [arXiv:astro-ph/0007362v1](#)
 Xu Z., 2021a, [arXiv e-prints](#), p. arXiv:2109.09985
 Xu Z., 2021b, [arXiv e-prints](#), p. arXiv:2109.12244
 Xu Z., 2021c, [arXiv e-prints](#), p. arXiv:2110.03126
 Xu Z., 2021d, [arXiv e-prints](#), p. arXiv:2110.05784

Table 2. List of data files in halo-based dataset for dark matter flow

Data file (*.csv)	Symbol	Reference	Eq.	Fig.
1_group_mass_m_g	m_g	(Xu 2021a)	(17)(56)	
2_group_number_of_halos_n_h	n_h	(Xu 2021a)	(35)	
3_mean_velocity_dispersion_sigma2_h	σ_h^2	(Xu 2021f)	(18)	2,3
4_particle_velocity_dispersion_sigma2_v	σ_v^2	(Xu 2021f)	(19)	2,4
5_mean_total_particle_potential	$\phi_v + \phi_h$	(Xu 2021f)	(52)	5,7,8
6_mean_intra_potential_phi	ϕ_v	(Xu 2021f)	(52)	5,7,8
7_mean_angular_velocity_omega_h	ω_h	(Xu 2021f)	(64)	15
8_mean_radial_moment_peculiar_G_hp	G_{hp}	(Xu 2021f)	(56)(to(58)	12
9_mean_radial_momentum_with_Hubble_flow_G_h	G_h	(Xu 2022c)	(102)	
10_mean_angular_momentum_H_h	H_h	(Xu 2021f)	(56)(to(58)	12
11_mean_radial_kinetic_energy_peculiar_K_rp	K_{rp}	(Xu 2021f)	(65)	16
12_mean_radial_kinetic_energy_with_Hubble_flow_K_r	K_r	(Xu 2022c)	(108)	
13_mean_rotational_kinetic_energy_K_a	K_a	(Xu 2021f)	(66)	16
14_mean_gamma_g_for_size	γ_g	(Xu 2022d)	(43)(55)	2
15_std_gamma_g_for_size	$\text{std}(\gamma_g)$	(Xu 2022d)	(43)(55)	2
16_mean_gamma_h_for_virial_ratio_of_halos	γ_h	(Xu 2021f)	(53)	6
17_mean_gamma_phi_for_potential_energy	γ_ϕ	(Xu 2022d)	(51)(55)	2
18_std_gamma_phi_for_potential_energy	$\text{std}(\gamma_\phi)$	(Xu 2022d)	(51)(55)	2
19_mean_alphas_for_potential_and_kinetic_energy	α_s^*	(Xu 2022d)	(53)	2
20_std_alphas_for_potential_and_kinetic_energy	$\text{std}(\alpha_s^*)$	(Xu 2022d)	(53)	2
21_mean_beta_s_for_radial_and_circular_velocity	β_s^*	(Xu 2022d)	(53)	2
22_std_beta_s_for_radial_and_circular_velocity	$\text{std}(\beta_s^*)$	(Xu 2022d)	(53)	2
23_mean_z_s_for_energy	z_s^*	(Xu 2022d)	(68)(69)	5
24_std_z_s_for_energy	$\text{std}(z_s^*)$	(Xu 2022d)	(68)(69)	5
25_mean_spin_parameter_lambda_p	λ_p	(Xu 2022d)	(70)(71)	6
26_std_spin_parameter_lambda_p	$\text{std}(\lambda_p)$	(Xu 2022d)	(70)(71)	6
27_mean_shape_parameter_h_e	h_e	(Xu 2021f)	(71)	20,21
28_std_shape_parameter_h_e	$\text{std}(h_e)$	(Xu 2021f)	(71)	20,21
29_mean_shape_parameter_h_p	h_p	(Xu 2021f)	(71)	20,21
30_std_shape_parameter_h_p	$\text{std}(h_p)$	(Xu 2021f)	(71)	20,21
31_mean_yita_s_for_angular_momentum	η_s^*	(Xu 2022d)	(62)(63)	6
32_std_yita_s_for_angular_momentum	$\text{std}(\eta_s^*)$	(Xu 2022d)	(62)(63)	6
33_mean_tau_s_for_radial_momentum	τ_s^*	(Xu 2022d)	(62)(63)	6
34_std_tau_s_for_radial_momentum	$\text{std}(\tau_s^*)$	(Xu 2022d)	(62)(63)	6
35_mean_root_mean_square_radius_r_g	r_g	(Xu 2021f)	(59)(to(61)	13,19
36_std_root_mean_square_radius_r_g	$\text{std}(r_g)$	(Xu 2021f)	(59)(to(61)	13,19
37_mean_radius_of_gyration_r_rg	r_{rg}	(Xu 2021f)	(63)(64)	
38_std_radius_of_gyration_r_rg	$\text{std}(r_{rg})$	(Xu 2021f)	(63)(64)	
39_mean_potential_exponent_n_s_for_virial_ratio_in_halos	$n_s = -\gamma_v$	(Xu 2021f)	(53)	6
40_std_potential_exponent_n_s_for_virial_ratio_in_halos	$\text{std}(n_s)$	(Xu 2021f)	(53)	6
41_mean_three_principal_semiaxis_length_lambda_r	$r_{\lambda 1,2,3}$	(Xu 2021f)	(67)(to(69)	19
42_mean_cos_angles_between_spin_axis_and_principal_axis	$\cos(\theta_{Hr})$	(Xu 2021f)		22
43_mean_inter_root_mean_square_velocity	v_{hg}	(Xu 2022g)	(7)(8)	5,6,7
44_mean_intra_root_mean_square_velocity	v_{hg}^i	(Xu 2022g)	(7)(8)	5,6,7
45_mean_total_root_mean_square_velocity	v_{hp}	(Xu 2022g)	(7)(8)	5,6,7
46_mean_inter_root_mean_square_acceleration	a_{hg}	(Xu 2022g)	(7)(8)	5,6,7
47_mean_intra_root_mean_square_acceleration	a_{hg}^i	(Xu 2022g)	(7)(8)	5,6,7
48_mean_total_root_mean_square_acceleration	a_{hp}	(Xu 2022g)	(7)(8)	5,6,7
49_mean_particle_pair_number_0.1Mpc_h	n_{pair}	(Xu 2022e)	(68)	
50_mean_particle_density_contrast_delta	δ			
51_mean_particle_logdensity_yita	η			
52_composite_halo_np=4_particle_data_z0	u_r, u_ϕ, u_θ	(Xu 2022c)		2,3
53_composite_halo_np=10_particle_data_z0	u_r, u_ϕ, u_θ	(Xu 2021b)		8,9,10
54_composite_halo_np=20_particle_data_z0	u_r, u_ϕ, u_θ	(Xu 2022c)		2,3
55_composite_halo_np=40_particle_data_z0	u_r, u_ϕ, u_θ	(Xu 2021b)		8,9,10
56_composite_halo_np=80_particle_data_z0	u_r, u_ϕ, u_θ	(Xu 2022c)		2,3
57_all_pairs_in_halo_z0_r_0.1Mpc_h	$\mathbf{r}, \mathbf{u}, \mathbf{u}', n_P$	(Xu 2021d)	(123)	7,8

Xu Z., 2021e, [arXiv e-prints](#), p. arXiv:2110.09676

Xu Z., 2021f, [arXiv e-prints](#), p. arXiv:2110.13885

Xu Z., 2022a, A comparative study of dark matter flow & hydrodynamic turbulence and its applications, [doi:10.5281/zenodo.6569902](#), [http://dx.doi.org/10.5281/zenodo.6569902](#)

Xu Z., 2022b, Dark matter flow dataset Part II: Correlation-based statistics from cosmological N-body simulation, [doi:10.5281/zenodo.6569899](#), [http://dx.doi.org/10.5281/zenodo.6569899](#)

Xu Z., 2022c, [arXiv e-prints](#), p. arXiv:2201.12665

Xu Z., 2022d, [arXiv e-prints](#), p. arXiv:2202.04054

Xu Z., 2022e, [arXiv e-prints](#), p. arXiv:2202.06515

Xu Z., 2022f, [arXiv e-prints](#), p. arXiv:2202.07240

Xu Z., 2022g, [arXiv e-prints](#), p. arXiv:2203.05606

Xu Z., 2022h, [arXiv e-prints](#), p. arXiv:2203.06899